

Cranfield



College of Aeronautics Report No.9012
July 1990

The Drag of Spheres at Porosities Ranging from an Isolated Sphere to a Packed Bed

J Pike

College of Aeronautics
Cranfield Institute of Technology
Cranfield, Bedford MK43 0AL. England



1401600911

Cranfield



College of Aeronautics Report No.9012
July 1990

The Drag of Spheres at Porosities Ranging from an Isolated Sphere
to a Packed Bed

J Pike

College of Aeronautics
Cranfield Institute of Technology
Cranfield, Bedford MK43 0AL. England

ISBN 1 871564 12 3

£8.00

*"The views expressed herein are those of the author alone and do not
necessarily represent those of the Institute"*

THE DRAG OF SPHERES AT POROSITIES RANGING FROM AN
ISOLATED SPHERE TO A PACKED BED

J. Pike

Cranfield Institute of Technology

Summary

It is suggested that the drag coefficient of spheres for Reynolds numbers up to 10^5 and a wide range of porosities is given approximately by

$$C_D = \epsilon^{-2.7} (C_{DS}(\epsilon Re) + \epsilon Re(1-\epsilon)(5\epsilon-2.2)/(100 + \epsilon Re))$$

where C_{DS} is the drag coefficient of an isolated sphere.

List of Symbols

A	cross section area of tube
A_p	cross section area of particle
C_D	drag coefficient
C_D^*	drag coefficient based on superficial velocity ϵu
C_{DS}	drag coefficient of an isolated sphere
C_R	$C_D Re/24 - 1$
D	drag
d	diameter of particle
d_p	diameter of particle
F_f	functions defined by eqs. (9) to (11)
L	length
N_{Re}	Reynolds number based on superficial velocity ϵu
n_p	number of particles in length L of tube
p	pressure
Re	Reynolds number
u	velocity
ω	$\log_{10} Re$
ϵ	porosity or void fraction
ρ	density
Δp	pressure difference
μ	viscosity

Introduction

Empirical relationships for the drag of spheres in the proximity of other spheres are available from fluid bed data [1]. These relationships have been developed for Reynolds numbers up to 10^3 and give large errors if used at higher Reynolds numbers. For applications such as the interior ballistics of guns, the drag at Reynolds numbers of up to 10^5 is needed. Here we attempt to extend the drag expressions to these higher Reynolds numbers.

Although the report is confined to spherical particles, for fluid beds and other applications, the particles of interest may not be spherical. The drag of non-spherical particles is usually related to the spherical particle drag by defining an "equivalent" spherical particle. For Reynolds numbers up to 10^3 it is suggested [1] that equivalent sphere should have the same surface area. Such an equivalence could form the basis of drag estimation of non-spherical particles up to Reynolds numbers of 10^5 , but its limitations would need investigation. Even without this "equivalence" uncertainty, it must be appreciated that the extension of the drag to higher Reynolds numbers based on the limited information available necessarily leaves some uncertainty in the accuracy of the expression for the sphere drag. However, for some applications the accuracy of the drag estimate is not critical and any reasonable estimate will suffice. For example, in internal ballistic calculations, the drag on the particles only affects the position of the energy input to the flow and not its amount. Thus some error in the drag can be accommodated without significant loss of accuracy in the solution.

2. Extension of the sphere drag expression to $Re \leq 10^5$

The correlations which are available [1] for the drag of interacting spheres up to a Reynolds number of 10^3 , can give large errors if applied at higher Reynolds numbers. To obtain the drag at higher Reynolds numbers the expressions need to be modified so that they match the available data. That is, they should match the drag of isolated spheres when the porosity is unity, approximate to the fixed bed results when the porosity is about 0.4 and smoothly blend to the fluid bed data when the Reynolds number is less than 10^3 . The lack of data at Reynolds numbers of 10^5 for

intermediate porosities will still leave uncertainty in the drag estimate near these values however.

For an isolated spherical particle at low Mach numbers, accurate expressions for the drag are available over the whole Reynolds number range [2]. The drag coefficient is expressed as a piecewise fit to the data using coefficients ω and C_R , where these are given by $\log_{10} Re$ and $C_D Re/24-1$ respectively. That is

$$\begin{aligned}
 \log_{10} C_R &= -2.1072 + \omega && Re \leq 0.01 && (1) \\
 &= -0.8810 + 0.8200\omega - 0.0500\omega^2 && 0.01 < Re \leq 20 \\
 &= -0.7133 + 0.6305\omega && 20 < Re \leq 260 \\
 \log_{10} C_D &= 1.6435 - 1.1242\omega + 0.1558\omega^2 && 260 < Re \leq 1500 \\
 &= -2.4571 + 2.5558\omega - 0.9295\omega^2 + 0.1049\omega^3 && 1500 < Re \leq 1.2 \times 10^4 \\
 &= -1.9181 + 0.6370\omega - 0.0636\omega^2 && 1.2 \times 10^4 < Re \leq 4.4 \times 10^4 \\
 &= -4.3390 + 1.5809\omega - 0.1546\omega^2 && 4.4 \times 10^4 < Re \leq 3.38 \times 10^5 \\
 C_D &= 29.78 - 5.3\omega && 3.38 \times 10^5 < Re \leq 4.03 \times 10^5 \\
 &= -0.49 + 0.1\omega && 4.03 \times 10^5 < Re \leq 10^6 \\
 &= 0.19 - 8 \times 10^4 / Re && 10^6 < Re
 \end{aligned}$$

The drag of isolated spheres from these expressions is shown in fig.1. Although the curve shown is for small Mach numbers, the variation in the drag for Mach numbers up to 0.5 is very small [3] and can be neglected. At larger Mach numbers an appropriate correction can be applied [3], but only the low Mach number expression of equations (1) is used here.

The correlation of Wen and Yu [1] using fluid bed data, is not based on equation (1), but on the drag expression of Schiller and Naumann [4]. This is also plotted in fig.1 and can be seen to be close to equation (1) for Reynolds numbers up to 10^3 . The Wen and Yu correlation can be written as

$$C_D^* = \epsilon^{-4.7} (24/N_{Re} + 3.6/N_{Re}^{0.313}) \quad (2)$$

where C_D^* and N_{Re} are the drag coefficient and Reynolds number based on the "superficial" velocity, that is on $\epsilon(u_g - u_p)$, where u_g is the gas

velocity and u_p the particle velocity. When C_D and Re are made independent of the porosity, equation (2) becomes

$$C_D = \epsilon^{-2.7} (24/(\epsilon Re) + 3.6/(\epsilon Re)^{0.313}) \quad (3)$$

The correlation between equation (2) or (3) and the data accumulated by Wen and Yu is shown in fig.2, taken from their paper [1]. The log scaling is such that a tenth of a vertical square represents and 25% change in the drag coefficient, suggesting a rapidly increasing error above Reynolds numbers of 10^3 . Wen and Yu comment on the error at Reynolds numbers of 10^3 , and suggest that using a more accurate estimate of the isolated sphere drag (i.e. when $\epsilon=1$) should reduce the error near these Reynolds numbers. Substituting the drag from equation (1) (with Re interpreted as ϵRe) in place of the bracketed expression in equation (3) does indeed reduce the error as is shown by the broken line in fig.2, but there is a clear indication that the drag needs to be even larger.

We now consider the fixed bed results. For a fixed bed of particles, the data and predictions are expressed as a pressure drop across a given length of bed. To use this data for our purposes, it is necessary to convert this pressure drop to a drag coefficient per spherical particle. The number of particles in a bed of length L and cross section area A is given from geometrical considerations by

$$n_p = \frac{6 L A (1-\epsilon)}{\pi d_p^3} \quad (4)$$

The loss of momentum across these particles is given by

$$n_p D = A \Delta p + A \Delta \rho u^2 \quad (5)$$

For small Mach numbers $\Delta \rho u^2$ may be neglected compared with Δp , so that

$$C_D = \frac{D}{\frac{1}{2} \rho u^2 A_p} = \frac{4 d_p}{3 \rho u^2 (1-\epsilon)} \frac{\Delta p}{L} \quad (6)$$

There have been a variety of correlations of fixed bed data for various Reynolds numbers and porosities. These are reviewed in references 5 and 6. The most established expression is that of Ergun [7] which is valid up to a Reynolds number of 2300 (1-ε). The correlation of Kuo and Nydegger [5] attempts to extend the Reynolds number to 23,500(1-ε), but it is based on data from beds with mixed particle shapes and sizes, making it difficult to know how to interpret the results. The more recent work of Jones and Krier [6] is more applicable and extends the fixed bed results to Reynolds numbers up to 10⁵.

These correlations can be written in the form [5]

$$\frac{\Delta p}{L} = \frac{\mu u}{d_p^2} \left(\frac{1-\epsilon}{\epsilon} \right)^2 F_f \quad (7)$$

$$= \frac{\rho u^2}{d_p \text{Re}} \left(\frac{1-\epsilon}{\epsilon} \right)^2 F_f \quad (8)$$

Where F_f is given by Ergun as

$$F_f = 150 + 1.75\epsilon \text{Re} / (1-\epsilon) \quad 0.4 \leq \epsilon \leq 0.65 \quad (9)$$

by Kuo and Nydegger as

$$F_f = 276.23 + 5.05(\epsilon \text{Re} / (1-\epsilon))^{0.87} \quad \epsilon \sim 0.38 \quad (10)$$

and by Jones and Krier as

$$F_f = 150 + 3.89(\epsilon \text{Re} / (1+\epsilon))^{0.87} \quad 0.38 \leq \epsilon \leq 0.44 \quad (11)$$

Using equation (6) we can write

$$C_D = \frac{4}{3\epsilon \text{Re}} \left(\frac{1-\epsilon}{\epsilon} \right) F_f \quad (12)$$

giving Ergun's relation for a sphere for example as

Using equation (6) we can write

$$C_D = \frac{4}{3\epsilon Re} \left(\frac{1-\epsilon}{\epsilon} \right) F_f \quad (12)$$

giving Ergun's relation for a sphere for example as

$$C_D = 25 \frac{(1-\epsilon)}{3\epsilon} \left(\frac{24}{\epsilon Re} + \frac{0.28}{1-\epsilon} \right) \quad (13)$$

These correlations are plotted in fig.3 for $\epsilon = 0.4$. This value of ϵ is outside the range for which the Kuo and Nydegger correlation was derived (i.e. ϵ from 0.376 to 0.390) but the higher drag for Reynolds numbers below 10^3 and the lower drag above 10^4 which they found is clearly illustrated.

Of greater interest is the extension of Ergun's correlation up to Reynolds numbers of 10^5 by Jones and Krier [6]. As shown in Fig.3, Jones and Krier predict a smaller drag at $\epsilon = 0.4$ than would be obtained by using Ergun's correlation extended up to 10^5 .

This extended Ergun correlation is compared with Wen and Yu's estimate [1] of the drag from fluid bed data in Fig.4. We see that at low porosity ($\epsilon = 0.4$) Wen and Yu's estimate is too large for Reynolds numbers less than 10^3 and too small for larger Reynolds numbers.

Also shown (by the broken line) on fig.4 is the modified Wen and Yu correlation, which can be expressed as

$$C_D = \epsilon^{-2.7} C_{DS}(\epsilon Re) \quad (14)$$

where C_{DS} is the isolated sphere drag given by equations (1). It can be seen that equation (14) gives a drag which is too high except for Reynolds numbers about 10^3 or very small Reynolds numbers.

At a slightly larger porosity of 0.44 (which is the largest value of ϵ for which the Jones and Krier correlation is valid), we see from Fig.5, that the agreement between the modified Wen and Yu and extended Ergun is improved, with large differences only occurring near Reynolds numbers of 10^5 .

In figs. 5 and 6 the modified Wen and Yu correlation is compared with Ergun's correlation for porosities of 0.5 and 0.6. We see that as the porosity increases, the difference between the correlations gets rapidly larger for Reynolds numbers above about 10^2 . Thus figs.5 and 6 (and also to some extent fig.2), suggest that better agreement could be obtained by adding a term which increased the drag in the intermediate porosity range for Reynolds numbers above 10^2 . We suggest the addition of a term of the form $k(\epsilon-0.44)(1-\epsilon)\epsilon Re/(100+Re)$ to C_{DS} in equation (14), which is zero when $\epsilon = 0.44$ or $\epsilon = 1$ and is small when ϵRe is less than 100. With the value of k put equal to 5, it is shown in fig.5 and 6, that the discrepancy with Ergun's correlation can be reduced for intermediate values of the porosity. Thus an expression of the form

$$C_D = \epsilon^{-2.7} (C_{DS}(\epsilon Re) + \epsilon Re(1-\epsilon)(5\epsilon-2.2)/(100 + \epsilon Re)) \quad 0 < Re < 10^5 \quad (15)$$

reduces to the isolated sphere drag coefficient when $\epsilon = 1$, is close to Ergun's correlation for $0.4 \leq \epsilon \leq 0.6$ and reduces to Wen and Yu's correlation for small Reynolds numbers.

In Appendix 1 the inclusion of buoyancy drag when using equation (15) is discussed. In Appendix 2 Fortran Functions for the drag coefficients given by equations (1) and (15) are given.

CONCLUSIONS

A drag expression is suggested for spheres which have porosities or void fractions of from 0.4 to 1, which is applicable for Reynolds numbers of up to 10^5 . The expression matches reliable data correlations for the drop of isolated spheres, the drag of spheres in packed beds and the drag of spheres at Reynolds numbers less than 10^3 . However the lack of data at intermediate porosities and Reynolds numbers of about 10^5 means that the estimate is not reliable in this region. There is a need for more data to improve the accuracy, but the estimate can be used for applications where great accuracy is not required.

References

1. Wen C.Y. and Yu Y.H. Mechanics of Fluidization, Chem. Eng. Prog. Symp. Ser. No.62, Vol.62, page 100, 1966.
2. Cliff R., Grace J.R. and Weber M.E. Bubbles, Drops and Particles, Academic Press, New York, 1978.
3. Henderson C.B. Drag coefficients of spheres in continuum and rarefied flows. AIAA J 14, 1976, pages 707-708.
4. Schiller L. and Naumann A. Z. Ver Deutsch Ing., 77, 318, 1935.
5. Kuo K.K. and Nydegger C.C. Flow Resistance Measurement and Correlation in a packed bed of WC870 Ball Propellants. Journal of Ballistics Vol.2, No.1, pages 1-25, 1978.
6. Jones D.P. and Krier H. Gas Flow Resistance Measurements Through Packed Beds at High Reynolds Numbers. Journal of Fluid Engineering. Transactions of the ASME Vol. 105, pages 168-173. June 1983.
7. Ergun S. Fluid Flow through Packed Columns. Chem. Engr. Progress, Vol.48, No.2, page 89, February 1952.

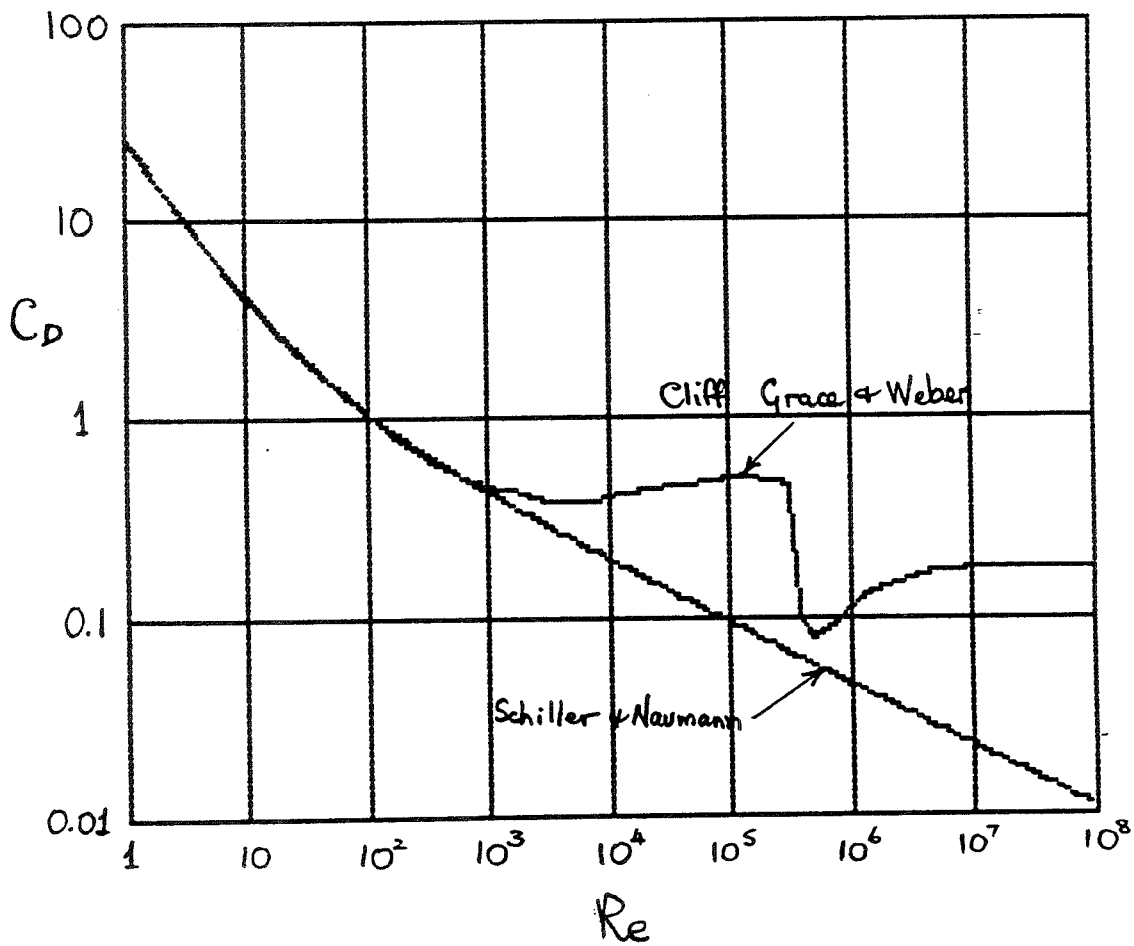


Fig.1: Drag coefficient of a sphere for a range of Reynolds numbers.

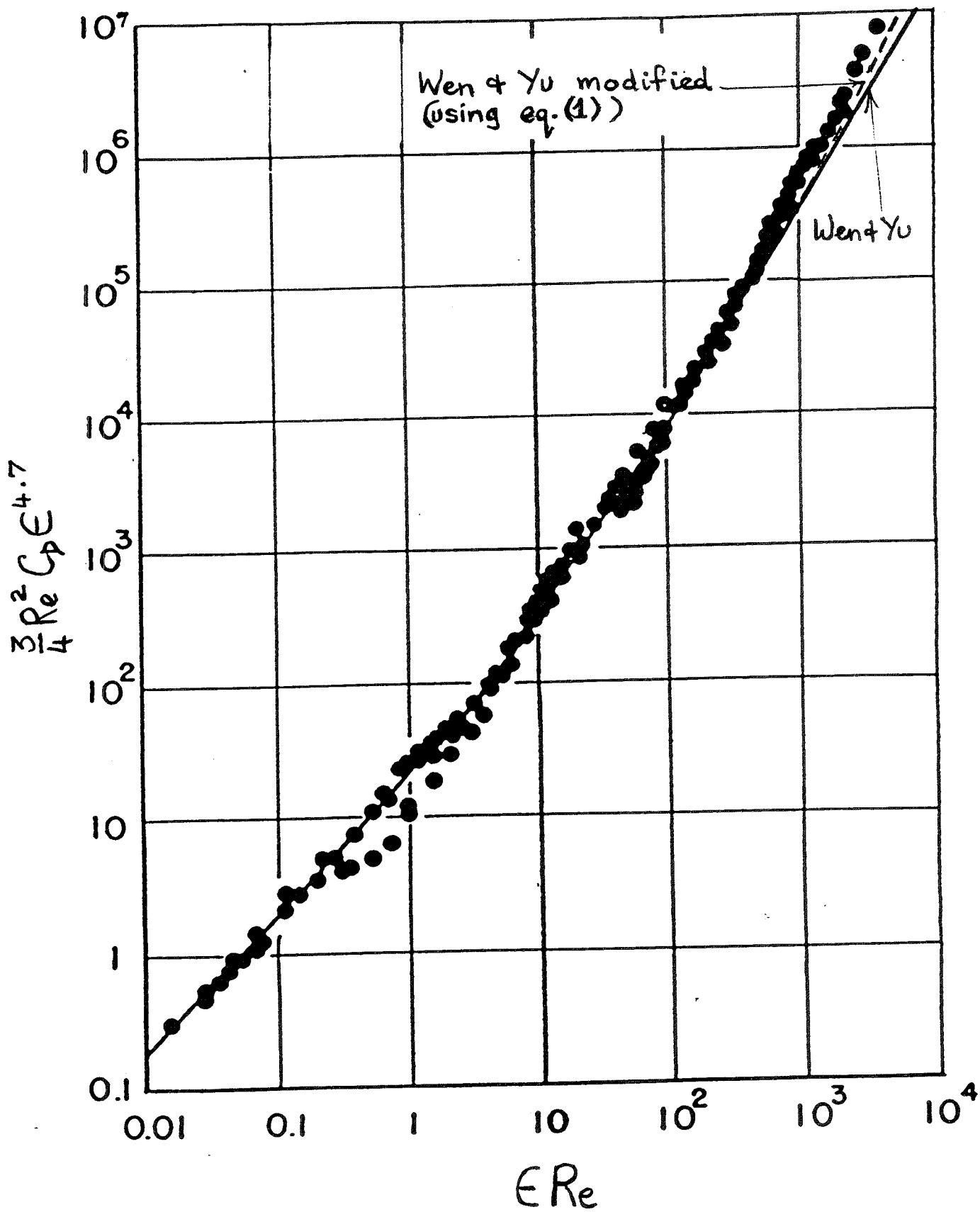


Fig.2: Generalized correlation for the bed expansion of spheres in a particulate fluidization (after Wen and Yu).

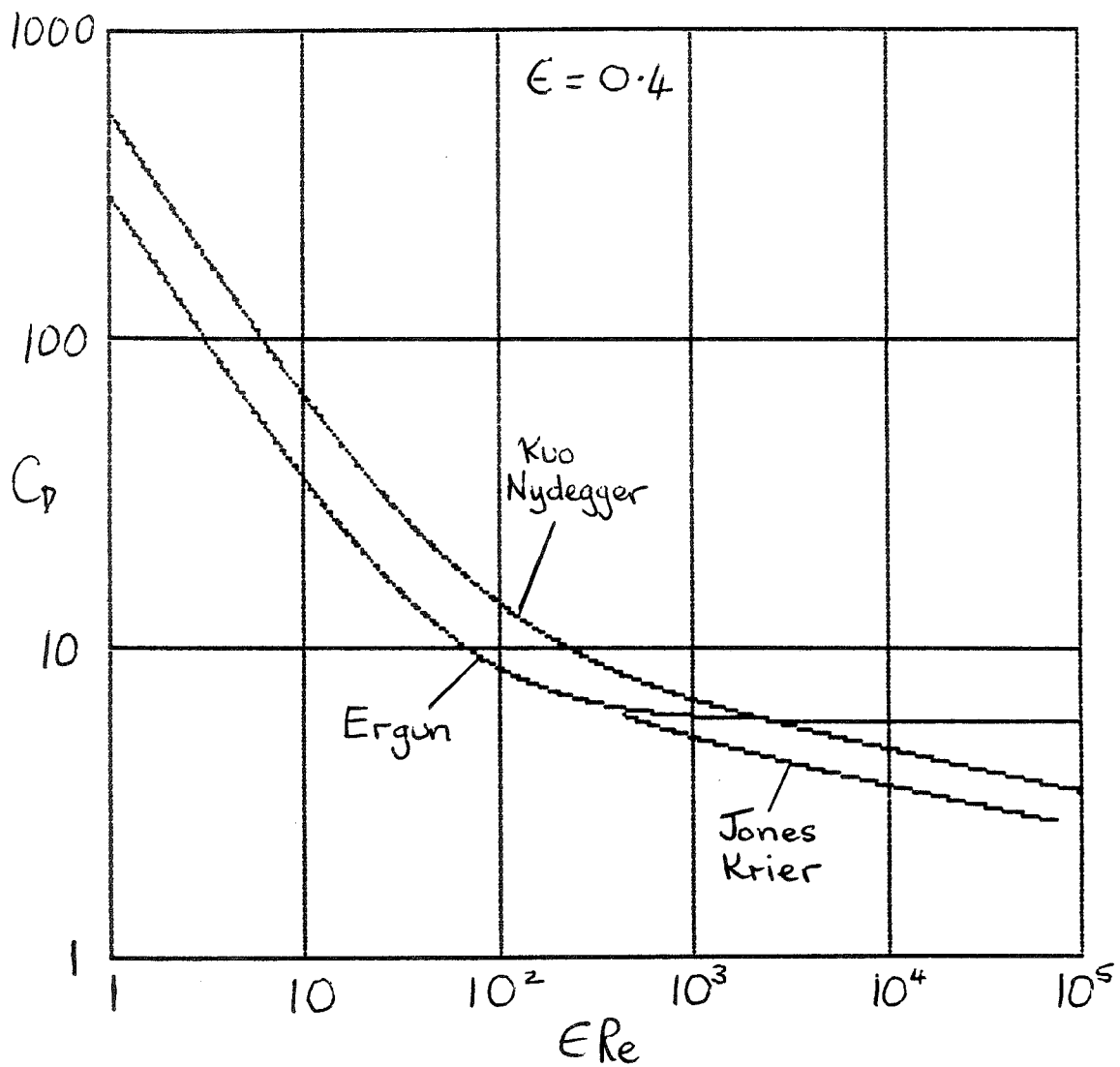


Fig.3: Drag coefficient of spheres from fixed bed data at a porosity of 0.4.

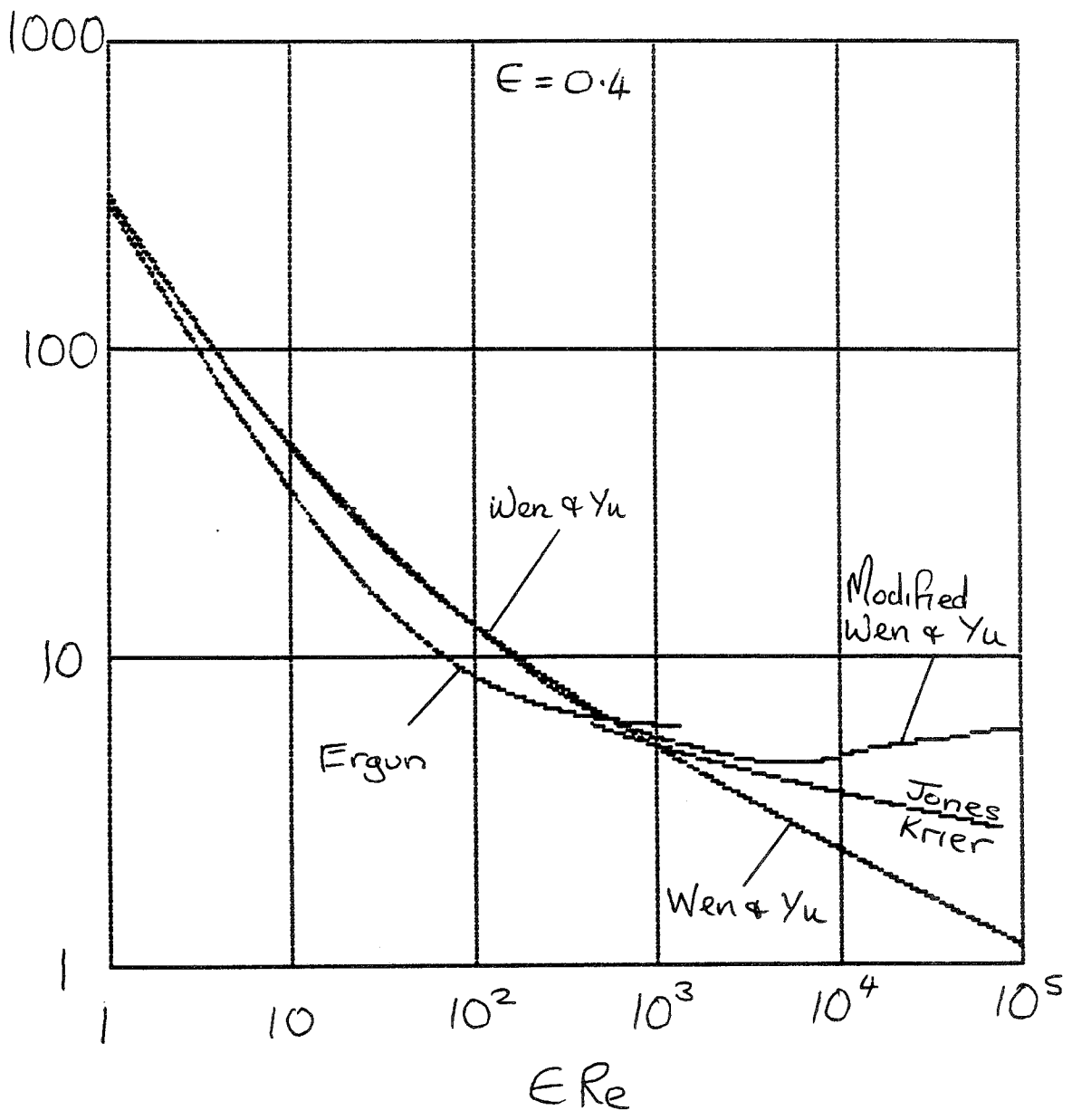


Fig.4 Comparison between fixed and fluid bed sphere drag correlations at a porosity of 0.4.

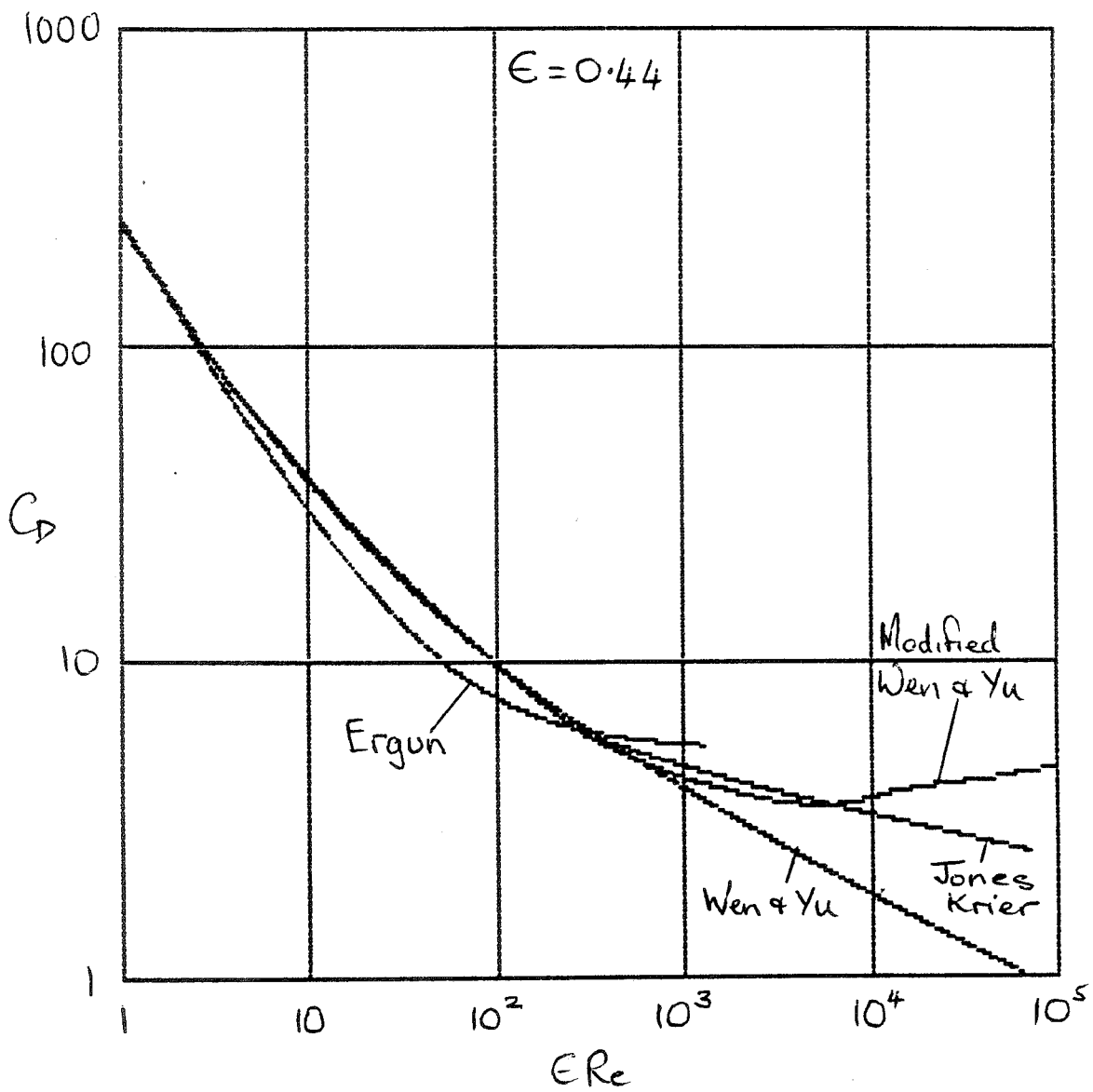


Fig.5 Comparison between fixed and fluid bed sphere drag correlations at a porosity of 0.44.

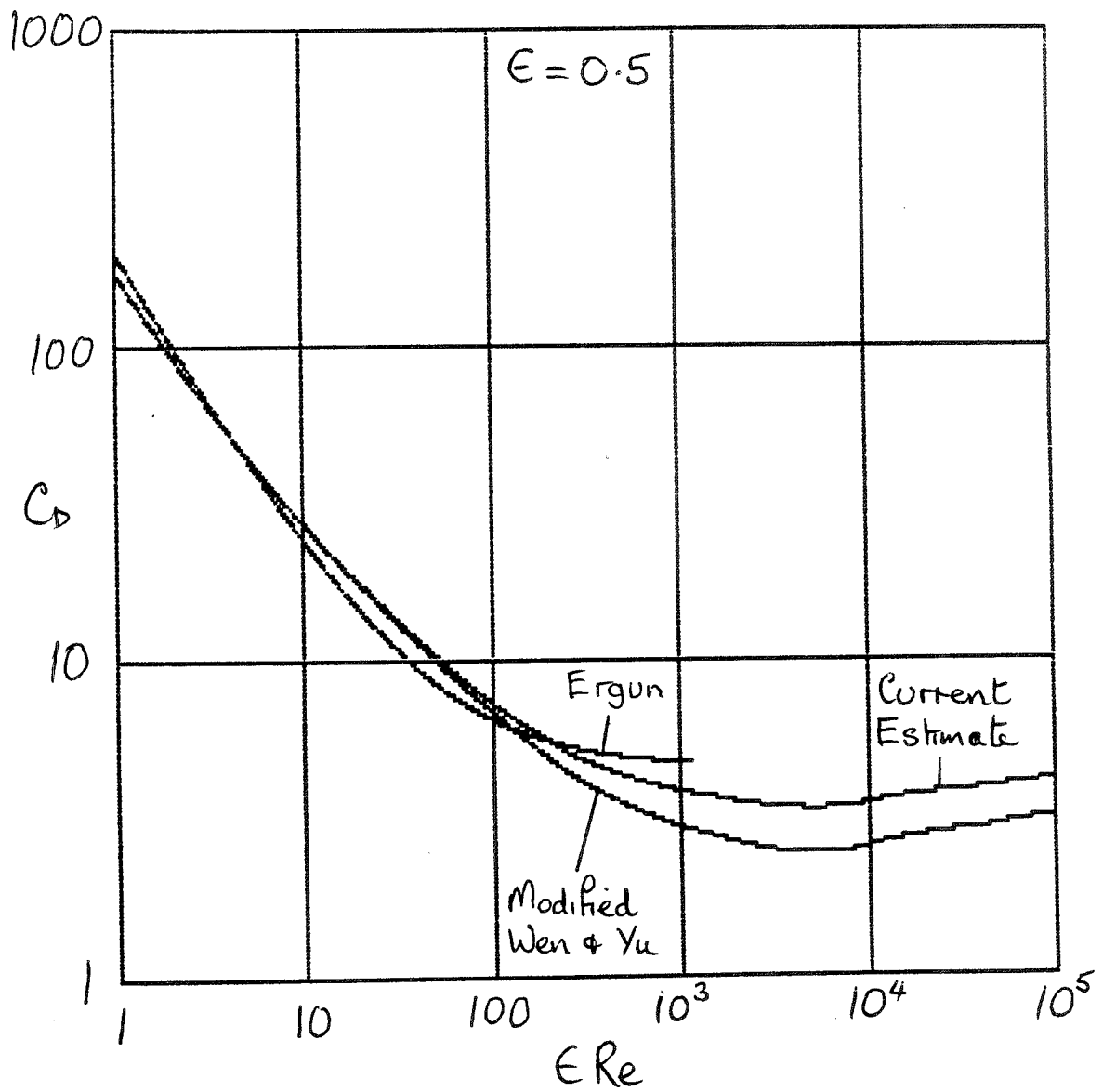


Fig.6 Drag coefficient of spheres at a porosity of 0.5.

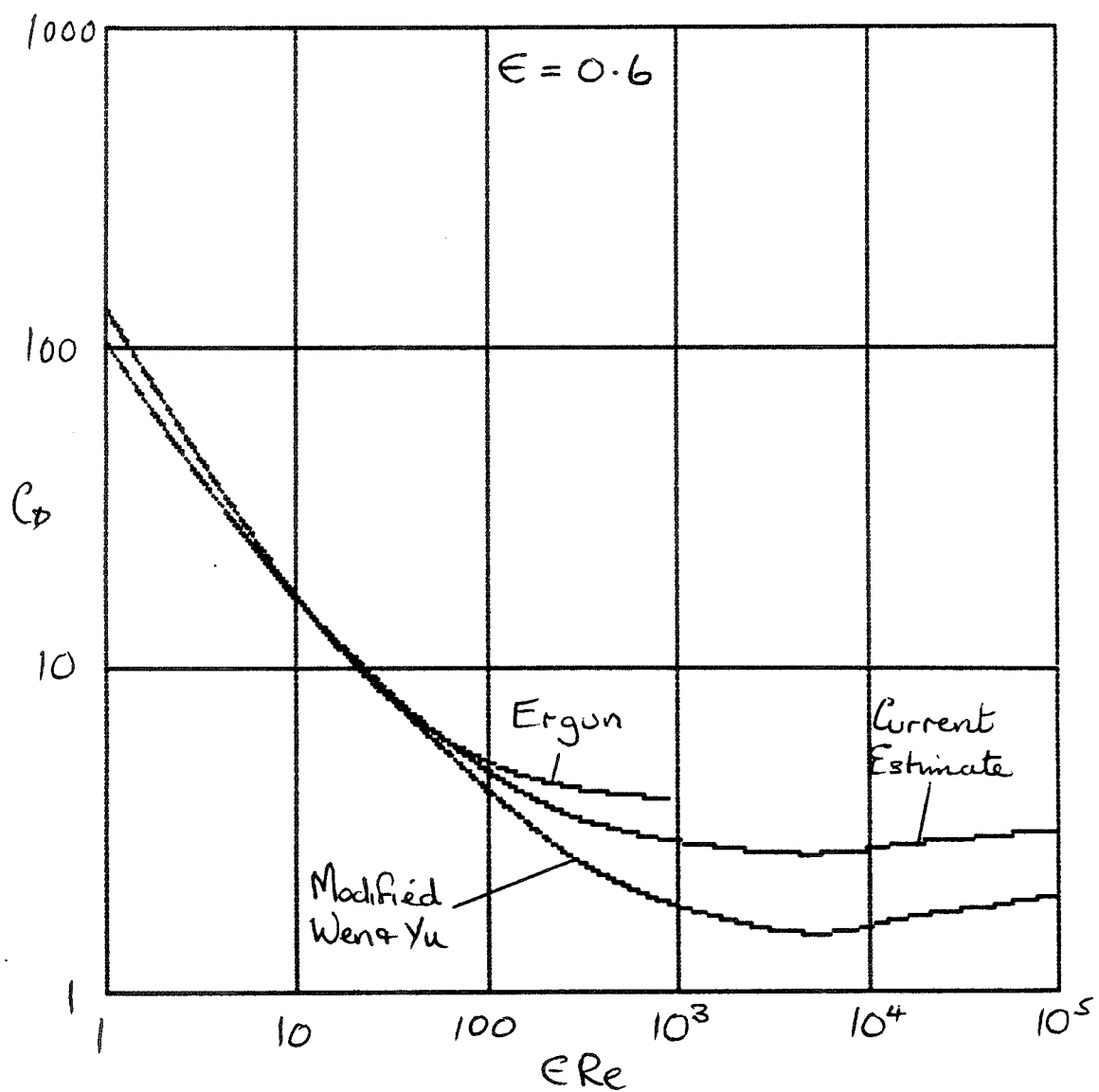


Fig.7 Drag coefficient of spheres at a porosity of 0.6.

APPENDIX 1

Application of drag expressions to tube calculations.

The drag of the particles in the flow includes the aerodynamic drag and the buoyancy. The former of these can be estimated using appropriate expressions, such as the drag expression developed here, where the velocity of the particles used to determine the Reynolds number is the relative velocity of the particles to the flow. The buoyancy drag depends on the particle volume and the pressure gradient. It should be noted that the aerodynamic drag of the particles will result in a pressure gradient and this should not be included in the buoyancy drag calculation. Thus the buoyancy drag is given by

$$\text{Particle Volume} \times \left(\frac{dp}{dx} - \frac{dp}{dx} (\text{aerodynamic drag}) \right)$$

The pressure gradient due to the aerodynamic drag can be obtained from a simple momentum balance as in equations (4) to (6).

APPENDIX 2

```

C DRAG COEFFICIENT OF SPHERE GIVEN VOID FRACTION AND RE<10**5
C VOID FRACTION OR POROSITY IS THE VOLUME FRACTION OF THE GAS SPACE
C REYNOLDS NUMBER RE=DENSITY GAS*SPHERE DIAM*RELATIVE VEL/VISCOSITY GAS
C ISOLATED SPHERE (VOID=1) VALID ALL RE (FORTRAN FUNCTION CDS(RE))
C MULTIPLE SPHERE (VOID<1) VALID RE<100,000 (J.PIKE,CRAFELD RPT 9012)
FUNCTION CDS(PHRE(VOID,RE)
  IF(VOID.LT.C.99.AND.RE.GT.1E5)WRITE(6,*)'INVALID CDS(PHRE,RE=',RE
  CDS(PHRE=VOID**(-2.7)*(CDS(RE)+VOID*RE*(1.0-VOID)*(5.0*VOID-2.2)/
  +(100.0+VOID*RE))
END

```

```

C DRAG COEFF OF SPHERE ANY REYNOLDS NUMBER
CLIFF,R GRACE,J.R WEBER,M.E; BUBBLES,DROPS & PARTICLES,ACADEMIC PRESS 78
C NB NEGATIVE VALLES OF RE (FROM NEG VEL) GIVE NEGATIVE CD!
FUNCTION CDS(RE)
  R=ABS(RE)
  C=0.0
  IF(R.EQ.0.0)GOTO 1
  W=LOG10(R)
  IF(R.GT.0.00 .AND.R.LE.0.01 ) C=LOG10(R/128.0)
  IF(R.GT.0.01 .AND.R.LE.20.0 ) C=-0.8810+0.8200*W-0.0500*W*W
  IF(R.GT.20.0 .AND.R.LE.260.0 ) C=-0.7133+0.6305*W
  IF(R.GT.260.0 .AND.R.LE.1500.0) C= 1.6435-1.1242*W+0.1558*W*W
  IF(R.GT.1.5E3 .AND.R.LE.1.2E4 ) C=-2.4571+2.5558*W-0.9295*W*W+
  +0.1049*W*W*W
  IF(R.GT.1.2E4 .AND.R.LE.4.4E4 ) C=-1.9181+0.6370*W-0.0636*W*W
  IF(R.GT.4.4E4 .AND.R.LE.3.38E5) C=-4.3390+1.5809*W-0.1546*W*W
  IF(R.GT.3.38E5 .AND.R.LE.4.03E5) C=29.7800-5.3000*W
  IF(R.GT.4.03E5 .AND.R.LE.1.0E6 ) C=-0.4900+0.1000*W
  IF(R.GT.1.0E6) C= 0.1900-8E4/R

```

```

C
  IF(R.LT.3.38E5)C=10**C
  IF(R.LT.260 )C=24/R*(1+C)
1 CDS=C*SIGN(1.0,RE)
END

```

